Dauphine | PSL UNIVERSITÉ PARIS
LEDa UMR 8007-260

LEDa WORKING PAPERS

Laurent series expansion for MA(∞) representation of mixed causal-noncausal autoregressive processes

Gilles De Truchis, Arthur Thomas

WP 2025-06

September 2025

Laurent series expansion for MA(∞) representation of mixed causal-noncausal autoregressive processes

Gilles de Truchis*, Arthur Thomas†

Abstract

This note develops a rigorous analytical framework for computing exact MA(∞) coefficients of mixed causal-noncausal autoregressive MAR(r, s). While analytical solutions exist only for the MAR(1, 1) specification in the existing literature (Gouriéroux and Jasiak, 2016), general MAR(r, s) processes are typically handled through recursive approximation algorithms that suffer from systematic truncation bias and numerical approximations. Using complex contour integration and the residue theorem, we derive explicit closed-form expressions valid for arbitrary orders (r, s). The derived expressions enable exact simulation algorithms and facilitate implementation of forecasting methodologies. Numerical comparisons with existing recursive methods demonstrate improvements in accuracy, and an experiment with α-stable innovations illustrate the empirical relevance of our results.

Keywords: Mixed causal-noncausal autoregression, Laurent series, Moving average representation, Complex analysis

MSC classes: 60G10, 60G52, 62M10

1 Introduction

Mixed causal-noncausal autoregressive processes have gained significant attention in the econometrics and time series analysis literature. Historically, the increasing attention devoted to these processes has been motivated by their utility in modeling complex temporal patterns in time series data, particularly explosive bubble phenomena in financial asset prices (Andrews et al., 2009; Lanne and Saikkonen, 2011; Gouriéroux and Jasiak, 2016; Gouriéroux and Zakoian, 2017; Velasco and Lobato, 2018; Hecq et al., 2020; Gourieroux and Jasiak, 2023; Hecq and Velasquez Gaviria, 2025; Blasques et al., 2025). These processes – characterized as the solution to rational expectations models with infinite variance innovations(Gourieroux et al., 2020a) – have also been investigated as a methodological approach to enhance macroeconometric modeling (Gouriéroux et al., 2020b). Furthermore, they have proven to be an effective analytical tool for modeling climate variables associated with extreme weather phenomena, including, for example, global temperature anomalies and ocean oscillation indices (Giancaterini et al., 2022; de Truchis et al., 2025). These processes, denoted MAR(r, s), are defined by the equation

$$\Phi(L)\Psi(L^{-1})y_t = \varepsilon_t \tag{1.1}$$

where $\Phi(L) = 1 - \phi_1 L - \phi_2 L^2 - \cdots - \phi_r L^r$ is the causal polynomial of order r, $\Psi(L^{-1}) = 1 - \psi_1 L^{-1} - \psi_2 L^{-2} - \cdots - \psi_s L^{-s}$ is the noncausal polynomial of order s, and ε_t is an independent and identically distributed (i.i.d.) heavy-tailed sequence. This representation is the one that is mostly used in the univariate case for simulation, estimation and prediction (Andrews et al., 2009; Lanne and Saikkonen, 2011; Gouriéroux and Jasiak, 2016; Hecq et al., 2020; Gourieroux and Jasiak, 2023). However, under some hypotheses detailed in Assumption 1, there is an equivalent to this multiplicative representation which is the moving average infinity MA(∞) representation

$$y_t = \frac{1}{\Phi(L)\Psi(L^{-1})} = \sum_{k\in\mathbb{Z}} \delta_k \varepsilon_{t+k} \tag{1.2}$$

*Université d'Orléans, Laboratoire d'Economie d'Orléans (LEO), 45000 Orléans, FRANCE, gilles.detruchis@univ-orleans.fr.
†Université Paris Dauphine, Université PSL, LEDA, CNRS, IRD, 75016 PARIS, FRANCE, arthur.thomas@dauphine.psl.eu.

where $(\delta_k)_{k\in\mathbb{Z}}$ is a deterministic coefficients sequence. This representation is also used for simulation and forecasting. Fries (2022) demonstrates that the $(\delta_k)_{k\in\mathbb{Z}}$ coefficients are essential for computing predictive conditional moments of mixed causal-noncausal ARMA processes. In an extension of this work, de Truchis et al. (2025) shows that during extreme events, conditional on observing a segment of the trajectory, mixed causal-noncausal processes are likely to be collinear to the $(\delta_k)_{k\in\mathbb{Z}}$ coefficients. However, few papers propose solutions to compute these coefficients. Gouriéroux and Jasiak (2016) suggest an approach based on partial fraction decomposition, as it allows theoretical derivation of an exact representation of the MA coefficients. However, the partial fraction decomposition can be tedious to derive for high-order (r, s) specifications, and the case $r = s = 1$ is essentially the only one considered in the literature. For large values of (r, s), existing approaches are typically based on recursive computation, similar to impulse response calculations. For example, this is the approach used in Lanne and Saikkonen (2011)'s seminal paper, extended in Hecq et al. (2020) and implemented in the so-called MARX package developed by Hecq et al. (2017). Unfortunately, this recursive approach introduces systematic truncation bias in coefficient computation, as it relies on defining the filtered components through $u_t \equiv \Phi(L)y_t$ and $v_t \equiv \Psi(L^{-1})y_t$ or equivalently $\Psi(L^{-1})u_t = \varepsilon_t$ and $\Phi(L)v_t = \varepsilon_t$ and there associated MA(∞) representation

$$u_t = \sum_{k=0}^{\infty} \delta_k^{(u)} \varepsilon_{t+k} \text{ and } v_t = \sum_{k=0}^{\infty} \delta_k^{(v)} \varepsilon_{t-k}$$

where $(\delta_k^{(u)})_{k\in\mathbb{Z}}$ and $(\delta_k^{(v)})_{k\in\mathbb{Z}}$ are coefficients of $[\Psi(L^{-1})]^{-1}$ and $[\Phi(L)]^{-1}$. The truncation bias arises from the approximation of the infinite sum, where ∞ is replaced by $m \in \mathbb{N}$.

This note extends the MAR(1,1) analytical result by deriving explicit closed-form expressions for the MA(∞) coefficients of any MAR(r, s) processes using complex analytic techniques. The remainder of this note is organized as follows. Section 2 presents the main lemma and associated proof. Section 3 applies this framework to several cases, including MAR$(1, 1)$, MAR$(1, 2)$ with complex conjugate noncausal roots, and MAR$(2, 3)$, with comparisons to recursive approximation methods. Section 4 presents exact simulation algorithms and shows how these coefficients can be used in a pattern-based forecasting methodology for processes with α-stable innovations. Section 5 concludes.

2 Theoretical results

For the analysis of the MA(∞) representation, it is convenient to express the autoregressive polynomials in their factorized forms in terms of their roots. The causal polynomial can be written as

$$\Phi(z) = 1 - \sum_{k=1}^{r} \phi_k z^k = \prod_{i=1}^{r} (1 - \lambda_i z)$$

and the noncausal polynomial as

$$\Psi(z^{-1}) = 1 - \sum_{k=1}^{s} \psi_k z^{-k} = \prod_{j=1}^{s} (1 - \zeta_j z^{-1}) = z^{-s} \prod_{j=1}^{s} (z - \zeta_j)$$

where λ_i and ζ_j represent the coefficients after factorization of the polynomials $\Phi(z)$ and $\Psi(z^{-1})$ respectively. In view of application of the residue theorem of Ahlfors (1979), we introduce the following Assumption.

Assumption 1 *Consider the process defined in Equation (1.2):*

(ι) *the innovations sequence ε_t is i.i.d with $\mathbb{E}(\varepsilon_t) = 0$.*

($\iota\iota$) *ε_t is regularly varying with tail index $\alpha > 0$ such that $\mathbb{E}(|\varepsilon_1|) < \infty$ if $\alpha > 1$ and $\mathbb{E}(|\varepsilon_1|^\beta) < \infty$ for some $\beta < \alpha$ if $\alpha \leq 1$*

($\iota\iota\iota$) *the coefficients sequence* $(\delta_k)_{k\in\mathbb{Z}}$ *is real-valued and satisfies*

$$\begin{cases} \sum_{k\in\mathbb{Z}} \delta_k^2 < \infty, & \text{if } \alpha > 2 \\ \sum_{k\in\mathbb{Z}} |\delta_k|^\beta < \infty, \quad \beta < \alpha, & \text{if } 0 < \alpha \leq 2 \end{cases} \tag{2.1}$$

such that the MA(∞) *representation of* (1.1) *converges a.s. for all* $t \in \mathbb{Z}$. *Also, under* ($\iota\iota\iota$), *for all* $i \in \{1,\dots,r\}$ *and* $j \in \{1,\dots,s\}$, r *and* s *finite, we assume :*

(ιv) $\mathcal{R}_1 = \max_{j=1,\dots,s} |\zeta_j| < 1$, $\mathcal{R}_2 = \min_{i=1,\dots,r} |\lambda_i|^{-1} > 1$, $\mathcal{R}_1 < \mathcal{R}_2$ *and define* $\mathcal{A} = \{z \in \mathbb{C} : \mathcal{R}_1 < |z| < \mathcal{R}_2\}$.

Assumption 1 provides sufficient conditions for the existence and convergence of the MA(∞) representation (1.2). The tail conditions in ($\iota\iota$) align with the non-causal literature requiring non-Gaussian errors for identification of anticipative roots but are unnecessary to apply the residue theorem. By contrast, (ιv) ensures convergence of the Laurent series in the annulus $\mathcal{A}$, which is essential for the application of the residue theorem and the demonstration of the following Lemma.

Lemma 2.1 *For a MAR*(r,s) *process defined by equation* (1.1) *with factorized polynomials* $\Phi(z) = \prod_{i=1}^r (1-\lambda_i z)$ *and* $\Psi(z^{-1}) = \prod_{j=1}^s (1-\zeta_j z^{-1})$ *satisfying Assumption 1, the MA*(∞) *coefficients of equation* (1.2) *are given by:*

(ι) *For* $k > 0$ *(noncausal coefficients):*

$$\delta_k = \sum_{j=1}^{s} \frac{\zeta_j^{(s-1)+k}}{\prod_{m\neq j}^s (\zeta_j - \zeta_m) \cdot \prod_{i=1}^r (\lambda_i \zeta_j - 1)} \cdot (-1)^r \tag{2.2}$$

($\iota\iota$) *For* $k \leq 0$ *(causal coefficients):*

$$\delta_k = \sum_{i=1}^{r} \frac{\lambda_i^{(r-1)+|k|}}{\prod_{l\neq i}^r (\lambda_i - \lambda_l) \cdot \prod_{j=1}^s (\lambda_i \zeta_j - 1)} \cdot (-1)^s \tag{2.3}$$

Proof of Lemma 2.1. The proof uses Laurent series expansion combined with contour integration techniques from complex analysis. The transfer function of the MAR(r,s) process can be written as

$$H(z) = \frac{1}{\Phi(z)\Psi(z^{-1})} = \frac{z^s}{\prod_{i=1}^r (1-\lambda_i z) \cdot \prod_{j=1}^s (z-\zeta_j)}.$$

The MA(∞) representation seeks coefficients δ_k such that

$$y_t = \sum_{k=-\infty}^{\infty} \delta_k \varepsilon_{t+k} = H(z)\varepsilon_t$$

where $H(z) = \sum_{k=-\infty}^{\infty} \delta_k z^{-k}$ is the Laurent series expansion. According to Laurent series theory, the coefficients are given by

$$\delta_k = \frac{1}{2\pi i} \oint_C H(z) z^{k-1} dz$$

where C is an appropriate contour lying in $\mathcal{A}$. Given our mixed causal-noncausal framework, the Laurent series expansion requires careful consideration of the regions in which each part of the series converges. The function $H(z)$ has two types of poles: poles at $z = 1/\lambda_i$ for $i = 1,\dots,r$ (all outside the unit circle since $|\lambda_i| < 1$) and poles at $z = \zeta_j$ for $j = 1,\dots,s$ (all inside the unit circle since $|\zeta_j| < 1$). To compute the coefficients δ_k, we choose contours within the convergence annulus $\mathcal{A}$ depending on the value of k.

(ι) For $k > 0$ (non-causal coefficients), the integrand grows as $|z| \to \infty$, so we use a contour C_+ in the region $\{z \in \mathcal{A} : |z| > \mathcal{R}_1\}$ oriented counterclockwise and enclosing all poles ζ_j. In that case, we denote by $f_+(z)$ the integrand. By the residue theorem (Ahlfors, 1979) and under Assumption 1 we have

$$\delta_k = \frac{1}{2\pi i} \oint_{C_+} f_+(z) dz = \sum_{j=1}^{s} \text{Res}(f_+, \zeta_j).$$

We compute the residue at each pole ζ_j as follows

$$\text{Res}(f_+, \zeta_j) = \lim_{z\to\zeta_j}(z-\zeta_j)\cdot\frac{z^{s+k-1}}{\prod_{i=1}^r(1-\lambda_i z)\cdot\prod_{m=1}^s(z-\zeta_m)} = \frac{\zeta_j^{s+k-1}}{\prod_{i=1}^r(1-\lambda_i\zeta_j)\cdot\prod_{m\neq j}(\zeta_j-\zeta_m)}.$$

Note that the denominator $\prod_{i=1}^r(1-\lambda_i\zeta_j)$ can be rewritten as $(-1)^r\prod_{i=1}^r(\lambda_i\zeta_j-1)$, introducing a factor $(-1)^r$. Equation (2.2) follows.

($\iota\iota$) Now consider the case $k\leq 0$ (causal coefficients). Since the integrand decays as $|z|\to\infty$ for $k\leq 0$, the integral over a large circle vanishes. Using a contour C_- in the region $\{z\in\mathcal{A}:|z|<\mathcal{R}_2\}$, oriented clockwise when viewed from infinity, the residue theorem yields

$$\delta_k = \frac{1}{2\pi i}\oint_{C_-} f_-(z)dz = -\sum_{i=1}^r \text{Res}(f_-, 1/\lambda_i), \tag{2.4}$$

where $f_-(z)$ denotes the integrand in that causal case. To compute the residue at each pole $1/\lambda_i$, we note that $1-\lambda_i z = -\lambda_i(z-1/\lambda_i)$ and thus,

$$\text{Res}(f_-, 1/\lambda_i) = \lim_{z\to 1/\lambda_i}(z-1/\lambda_i)\cdot\frac{z^{s+k-1}}{\prod_{l=1}^r(1-\lambda_l z)\cdot\prod_{j=1}^s(z-\zeta_j)} = \lim_{z\to 1/\lambda_i}\frac{z^{s+k-1}}{(-\lambda_i)\prod_{l\neq i}(1-\lambda_l z)\cdot\prod_{j=1}^s(z-\zeta_j)}.$$

Substituting $z=1/\lambda_i$,

$$\text{Res}(f_-, 1/\lambda_i) = \frac{(1/\lambda_i)^{s+k-1}}{(-\lambda_i)\prod_{l\neq i}(1-\lambda_l/\lambda_i)\cdot\prod_{j=1}^s(1/\lambda_i-\zeta_j)}$$

and simplifying the denominators as

$$\prod_{l\neq i}(1-\lambda_l/\lambda_i) = \prod_{l\neq i}\frac{\lambda_i-\lambda_l}{\lambda_i} = \frac{\prod_{l\neq i}(\lambda_i-\lambda_l)}{\lambda_i^{r-1}}$$
$$\prod_{j=1}^s(1/\lambda_i-\zeta_j) = \prod_{j=1}^s\frac{1-\lambda_i\zeta_j}{\lambda_i} = \frac{\prod_{j=1}^s(1-\lambda_i\zeta_j)}{\lambda_i^s}$$

we obtain

$$\text{Res}(f_-, 1/\lambda_i) = \frac{\lambda_i^{-(s+k-1)}}{(-\lambda_i)\cdot\frac{\prod_{l\neq i}(\lambda_i-\lambda_l)}{\lambda_i^{r-1}}\cdot\frac{\prod_{j=1}^s(1-\lambda_i\zeta_j)}{\lambda_i^s}} = \frac{\lambda_i^{r-k-1}}{\prod_{l\neq i}(\lambda_i-\lambda_l)\cdot\prod_{j=1}^s(1-\lambda_i\zeta_j)}\cdot(-1).$$

We can rewrite the denominator $\prod_{j=1}^s(1-\lambda_i\zeta_j)$ as $(-1)^s\prod_{j=1}^s(\lambda_i\zeta_j-1)$, which gives

$$\text{Res}(f_-, 1/\lambda_i) = \frac{(-1)^{1-s}\lambda_i^{r-1-k}}{\prod_{l\neq i}(\lambda_i-\lambda_l)\cdot\prod_{j=1}^s(\lambda_i\zeta_j-1)}.$$

Since $k\leq 0$, we have $r-1-k=(r-1)+|k|$, yielding equation (2.3) once we accounted for the negative sign in Equation (2.4). □

3 Some particular processes

3.1 MAR(1,1) Case

In this section, we consider the known case from Gouriéroux and Jasiak (2016): a simple MAR$(1,1)$ process with $\Phi(L)=1-\phi L$ and $\Psi(L^{-1})=1-\psi L^{-1}$, so $\lambda_1=\phi$ and $\zeta_1=\psi$. For our numerical exercise, we choose a MAR$(1,1)$ process with a causal coefficient $\phi=0.6$ and a noncausal coefficient $\psi=0.7$, which corresponds to $(1-0.6L)(1-0.7L^{-1})y_t=\varepsilon_t$. This process exhibits both causal and noncausal dynamics, with the causal component contributing moderate persistence

backward in time, and the noncausal component providing stronger persistence in the anticipatory effects forward in time. Applying the formulas from Lemma 2.1, we get for $k > 0$

$$\delta_k = \frac{\zeta_1^{(1-1)+k}}{\prod_{m\neq 1}^{1}(\zeta_1 - \zeta_m) \cdot \prod_{i=1}^{1}(\lambda_i \zeta_1 - 1)} \cdot (-1)^1 = \frac{\psi^k}{1 - \phi\psi}.$$

The central coefficient is obtained by taking the limit or direct application,

$$\delta_0 = \frac{1}{1 - \phi\psi}$$

and we obtain for $k < 0$ from equation (2.3)

$$\delta_k = \frac{\lambda_1^{(1-1)+|k|}}{\prod_{l\neq 1}^{1}(\lambda_1 - \lambda_l) \cdot \prod_{j=1}^{1}(\lambda_1 \zeta_j - 1)} \cdot (-1)^1 = \frac{\phi^{|k|}}{1 - \phi\psi}.$$

For our specific values $\phi = 0.6$ and $\psi = 0.7$:

$$\begin{aligned}
\delta_k &= \frac{\psi^k}{1 - \phi\psi} = \frac{(0.7)^k}{0.58}, \quad k > 0 \\
\delta_0 &= \frac{1}{1 - \phi\psi} = \frac{1}{0.58} \approx 1.724 \\
\delta_k &= \frac{\phi^{|k|}}{1 - \phi\psi} = \frac{(0.6)^{|k|}}{0.58}, \quad k < 0
\end{aligned}$$

These results demonstrate the characteristic asymmetric decay pattern of MAR$(1,1)$ coefficients: the future coefficients δ_k for $k > 0$ decay at rate $\psi = 0.7$, while the past coefficients for $k < 0$ decay at the faster rate $\phi = 0.6$. The normalization factor $1/(1 - \phi\psi) = 1/0.58 \approx 1.724$ ensures proper scaling of the MA(∞) representation.

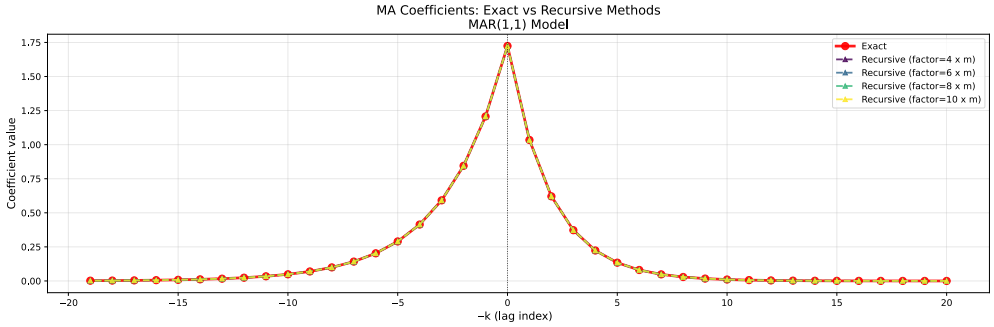

Figure 1: The $m = 20$ first MA(∞) coefficients δ_k for MAR$(1,1)$ process with $\phi = 0.6$ and $\psi = 0.7$. The graph compares our exact algorithm and the recursive method for different length factors used in the approximation.

The graphical analysis in Figure 1 reveals that the performance between our exact algorithm and the recursive method are comparable in this particular case. The two methods are very close because the exponential decay is preserved on both sides in the MAR(1,1) case. The curves show clear asymmetric decay around the central peak $\delta_0 \approx 1.724$. Past influences $(k < 0)$ decay geometrically at rate $\phi = 0.6$, while future influences $(k > 0)$ decay more slowly at rate $\psi = 0.7$. This temporal asymmetry manifests in the immediate neighbors: $\delta_{-1} \approx 1.034 < \delta_1 \approx 1.207$, indicating stronger anticipatory effects than backward-looking dynamics.

3.2 MAR(1,2) Case with complex conjugate noncausal roots

In this section, we examine a specific MAR$(1,2)$ process with causal coefficient $\phi_1 = 0.6$ and noncausal coefficients $\psi_1 = 0.8$ and $\psi_2 = -0.5$, which corresponds to the process $X_t = 0.6X_{t-1} + 0.8X_{t+1} - 0.5X_{t+2} + \varepsilon_t$. The general MAR$(1,2)$ process

is defined by $\Phi(L)\Psi(L^{-1})y_t = (1-\lambda_1 L)(1-\zeta_1 L^{-1})(1-\zeta_2 L^{-1})y_t = \varepsilon_t$. For the causal coefficient, we have $\lambda_1 = 0.6$, obtained directly from the first-order polynomial. For the noncausal roots ζ_1 and ζ_2, we solve the characteristic equation $z^2 - 0.8z + 0.5 = 0$. The discriminant is $\Delta = (0.8)^2 - 4(0.5) = 0.64 - 2.0 = -1.36 < 0$, yielding complex conjugate roots

$$\zeta_1 = \frac{0.8 + i\sqrt{1.36}}{2} = 0.4 + 0.583i \text{ and } \zeta_2 = \frac{0.8 - i\sqrt{1.36}}{2} = 0.4 - 0.583i$$

and hence $|\zeta_j| = \sqrt{(0.4)^2 + (0.583)^2} = \sqrt{0.16 + 0.340} = \sqrt{0.5} \approx 0.707 < 1$, $j = \{1, 2\}$. From Lemma 2.1, for $k > 0$, the coefficients are given by:

$$\delta_k = \frac{\zeta_1^{(s-1)+k}}{\prod_{m\neq 1}^{s}(\zeta_1 - \zeta_m)\cdot\prod_{i=1}^{r}(\lambda_i\zeta_1 - 1)}\cdot(-1)^r + \frac{\zeta_2^{(s-1)+k}}{\prod_{m\neq 2}^{s}(\zeta_2 - \zeta_m)\cdot\prod_{i=1}^{r}(\lambda_i\zeta_2 - 1)}\cdot(-1)^r = \frac{(-1)^r}{\zeta_1 - \zeta_2}\left[\frac{\zeta_1^{1+k}}{\lambda_1\zeta_1 - 1} - \frac{\zeta_2^{1+k}}{\lambda_1\zeta_2 - 1}\right]$$

Since $\zeta_1 - \zeta_2 = 2i\cdot\text{Im}(\zeta_1) = 2i(0.583) = 1.166i$, and using the complex conjugate properties with $\lambda_1 = 0.6$, we obtain

$$\delta_k = -\frac{1}{1.166i}\left[\frac{(0.4 + 0.583i)^{1+k}}{-0.76 + 0.350i} - \frac{(0.4 - 0.583i)^{1+k}}{-0.76 - 0.350i}\right].$$

For $k \leq 0$ we obtain

$$\delta_k = \sum_{i=1}^{1}\frac{\lambda_i^{(r-1)+|k|}}{\prod_{l\neq i}^{1}(\lambda_i - \lambda_l)\cdot\prod_{j=1}^{2}(\lambda_i\zeta_j - 1)}\cdot(-1)^s = \frac{\lambda_1^{|k|}}{(\lambda_1\zeta_1 - 1)(\lambda_1\zeta_2 - 1)}\cdot(-1)^2 = \frac{\lambda_1^{|k|}}{(\lambda_1\zeta_1 - 1)(\lambda_1\zeta_2 - 1)}$$

Replacing by the numerical values we obtain:

$$\delta_k = \frac{(0.6)^{|k|}}{(0.6\cdot(0.4 + 0.583i) - 1)(0.6\cdot(0.4 - 0.583i) - 1)} = \frac{(0.6)^{|k|}}{0.7}$$

And finally, for $k = 0$ we have

$$\delta_0 = \frac{1}{(\lambda_1\zeta_1 - 1)(\lambda_1\zeta_2 - 1)} = \frac{1}{0.7} \approx 1.429.$$

Figure 2 presents the MA(∞) coefficients for the mixed MAR(1, 2) process with $\phi_1 = 0.6$ and complex conjugate noncausal

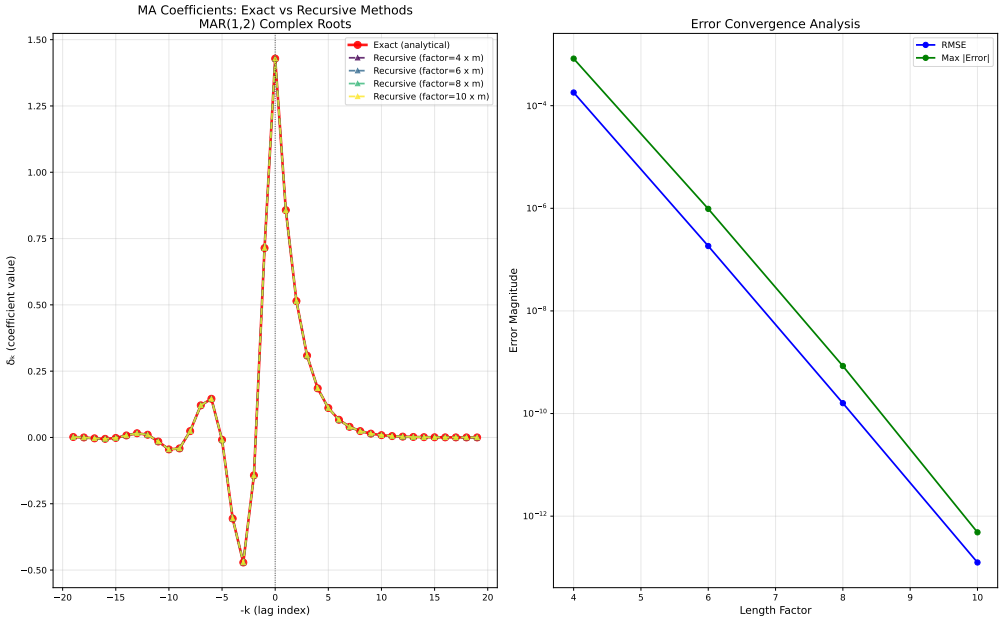

Figure 2: MA(∞) coefficients δ_k for MAR(1, 2) process with complex conjugate noncausal roots which corresponds to $\psi_1 = 0.8$, $\psi_2 = -0.5$ and $\phi_1 = 0.6$. The graph compares our exact algorithm and the recursive method for different length factors used in the approximation. On the right hand side, we also report the relative error convergence of the two methods in terms of relative RMSE and maximum absolute error.

roots $\zeta_1 = 0.4 + 0.583i$, $\zeta_2 = 0.4 - 0.583i$ ($\psi_1 = 0.8$, $\psi_2 = -0.5$). The coefficients exhibit asymmetric structure with positive central peak $\delta_0 \approx 1.429$. The backward component ($k < 0$) shows exponential decay at rate 0.6 with alternating signs, while the forward component ($k > 0$) displays oscillatory decay with envelope rate $\sqrt{0.5} \approx 0.707$. The recursive method exhibits reduced accuracy for complex conjugate roots, requiring higher truncation factors to achieve convergence.

3.3 MAR(2,3) Case

In this section, we examine a specific MAR$(2,3)$ process with causal coefficients $\phi_1 = 0.5$ and $\phi_2 = 0.3$, and noncausal coefficients $\psi_1 = 0.8$, $\psi_2 = 0.2$, and $\psi_3 = -0.1$, which corresponds to the process $X_t = 0.5X_{t-1} + 0.3X_{t-2} + 0.8X_{t+1} + 0.2X_{t+2} - 0.1X_{t+3} + \varepsilon_t$. The general MAR$(2,3)$ process is defined by $\Phi(L)\Psi(L^{-1})y_t = (1-\lambda_1 L)(1-\lambda_2 L)(1-\zeta_1 L^{-1})(1-\zeta_2 L^{-1})(1-\zeta_3 L^{-1})y_t = \varepsilon_t$. Solving the characteristic equation of the causal part we get $\lambda_1 = 0.852$ and $\lambda_2 = -0.352$. For the noncausal roots we obtain $\zeta_1 = 0.863$, $\zeta_2 = 0.087$, and $\zeta_3 = -0.150$. From our general formulas in Lemma 2.1, the coefficients are given by: For $k > 0$ applying equation (2.2), we get:

$$\delta_k = \sum_{j=1}^{3} \frac{\zeta_j^{2+k}}{\prod_{m\neq j}^{3}(\zeta_j - \zeta_m) \cdot \prod_{i=1}^{2}(\lambda_i \zeta_j - 1)}$$

For $k \leq 0$ applying equation (2.3) , we obtain the following results:

$$\delta_k = \sum_{i=1}^{2} \frac{\lambda_i^{1+|k|}}{\prod_{l\neq i}^{2}(\lambda_i - \lambda_l) \cdot \prod_{j=1}^{3}(\lambda_i \zeta_j - 1)} \cdot (-1)$$

The central coefficient δ_0 reflects the multiplicative interaction between all causal and noncausal roots:

$$\delta_0 = \frac{1}{\prod_{i=1}^{2}\prod_{j=1}^{3}(\lambda_i \zeta_j - 1)}$$

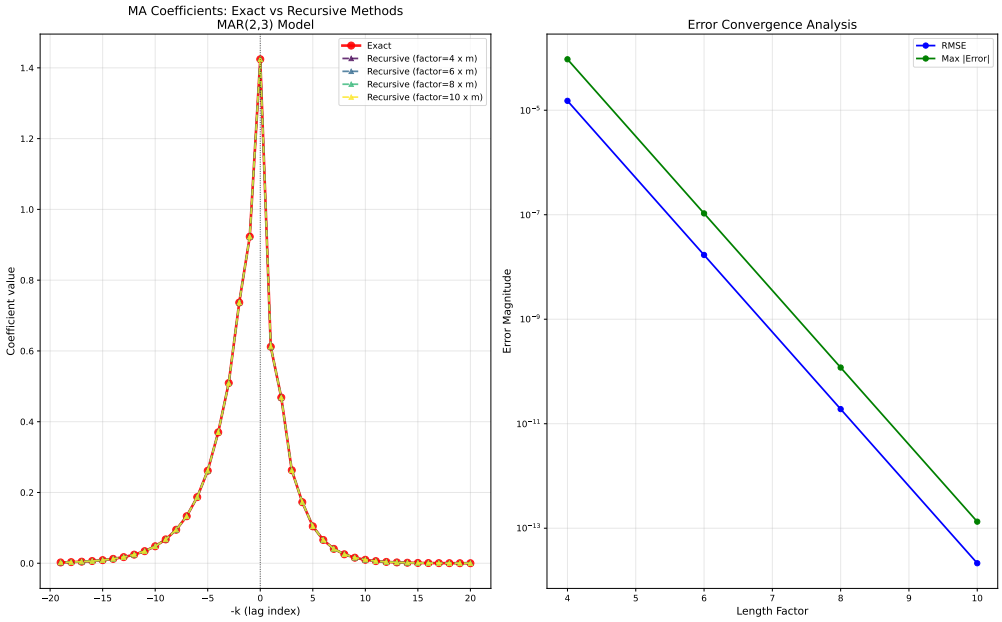

Figure 3: The $m = 20$ first MA(∞) coefficients δ_k for mixed MAR$(2,3)$ process with causal coefficients $\phi_1 = 0.5$, $\phi_2 = 0.3$ and noncausal coefficients $\psi_1 = 0.8$, $\psi_2 = 0.2$, $\psi_3 = -0.1$. The graph compares our exact algorithm and the recursive method for different length factors used in the approximation. On the right hand side, we also report the relative error convergence of the two methods in terms of relative RMSE and maximum absolute error.

Figure 3 presents the MA(∞) coefficients for the mixed MAR$(2,3)$ process. The curves reveal the sophisticated asymmetric structure characteristic of high-order mixed processes. The causal component ($k < 0$) exhibits sophisticated decay patterns from two causal roots: dominant $\lambda_1 = 0.852$ and oscillatory $\lambda_2 = -0.352$. The noncausal component ($k > 0$) also displays intricate decay from three roots: primary $\zeta_1 = 0.863$, secondary $\zeta_2 = 0.087$, and oscillatory $\zeta_3 = -0.150$. The central coefficient $\delta_0 \approx 1.42$ reflects the multiplicative interactions. Again, the recursive method displays lower precision than our exact approach.

4 Simulation and forecasting algorithms

Based on the closed-form expressions derived in Lemma 2.1, we present a direct simulation algorithm for MAR(r,s) processes. This method explicitly computes the MA(∞) coefficients to generate process realizations with controlled truncation error. Accordingly, the algorithm proceeds through the following steps:

(ι) *Coefficient computation*: using equations (2.2) and (2.3), we compute the MA(∞) coefficients δ_k for a sufficiently large range $k \in [-m, m]$, where m is chosen such that $|\delta_k| < \epsilon$ for some predetermined tolerance $\epsilon > 0$ and $|k| > m$.

($\iota\iota$) *Heavy-tailed innovation generation*: generate i.i.d. innovations ε_t following an α-stable distribution $S(\alpha, \beta, \sigma, \mu)$. The parameters control tail behavior ($\alpha \in (0,2]$), asymmetry ($\beta \in [-1,1]$), scale ($\sigma > 0$), and location ($\mu \in \mathbb{R}$). Other heavy-tailed distributions may be substituted as needed (Student t distribution)

($\iota\iota\iota$) *Process simulation*: for each time point $t \in \{m+1, \ldots, T-m\}$, compute the exact process values:

$$y_t = \sum_{k=-m}^{m} \delta_k \varepsilon_{t+k} \tag{4.1}$$

The explicit computation of the MA(∞) coefficients δ_k provides a theoretical foundation for advanced forecasting methods based on pattern recognition during extreme events (see e.g. Fries, 2022; de Truchis et al., 2025). As an illustration, consider a MAR$(1,3)$ process defined as the strictly stationary solution of

$$(1 - 0.8L^{-1})(1 - 0.6L)(1 - 0.3L)(1 - 0.1L)X_t = \varepsilon_t$$

where the noncausal root is $\zeta_1 = 0.8$ and the causal roots are $\lambda_1 = 0.6$, $\lambda_2 = 0.3$, $\lambda_3 = 0.1$. Here ε_t is an i.i.d. sequence of regularly varying errors with tail index $\alpha = 1.5$. The process (X_t) admits the MA(∞) representation $X_t = \sum_{k\in\mathbb{Z}} \delta_k \varepsilon_{t+k}$ with coefficients computed via Lemma 2.1. Following Fries (2022), denote $\mathbf{X}_t := (X_{t-m}, \ldots, X_t)$, $\mathbf{X}_{t+h} := (X_{t+1}, \ldots, X_{t+h})$, and define the forecasting patterns

$$\mathbf{D}_k := \frac{(\delta_{k-1}, \delta_{k-2}, \ldots, \delta_{k-h})}{|\delta_k|} \quad \text{for } k \in \{0, 1, \ldots, h\}.$$

From Lemma 2.1, for $k > 0$, we obtain

$$\delta_k = \frac{\zeta_1^{(s-1)+k}}{\prod_{i=1}^{3}(\lambda_i\zeta_1 - 1)} \cdot (-1)^r = \frac{(0.8)^{0+k}}{(0.6 \times 0.8 - 1)(0.3 \times 0.8 - 1)(0.1 \times 0.8 - 1)} \cdot (-1)^3$$

Computing the denominator

$$(0.48 - 1)(0.24 - 1)(0.08 - 1) = (-0.52)(-0.76)(-0.92) = -0.363584.$$

Therefore, for $k \geq 0$, $\delta_k = \frac{-1\times(0.8)^k}{-0.363584} = 2.750(0.8)^k$, yielding $\delta_0 = 2.750$, $\delta_1 = 2.200$, $\delta_2 = 1.760$, $\delta_3 = 1.408$. For $k < 0$, we get

$$\delta_k = \sum_{i=1}^{3} \frac{\lambda_i^{(r-1)+|k|}}{\prod_{l\neq i}^{3}(\lambda_i - \lambda_l) \cdot (\lambda_i\zeta_1 - 1)} \cdot (-1)^s = \sum_{i=1}^{3} \frac{\lambda_i^{2+|k|}}{\prod_{l\neq i}^{3}(\lambda_i - \lambda_l) \cdot (\lambda_i\zeta_1 - 1)} \cdot (-1)$$

By computing each term, we obtain:

$$\delta_k = \frac{(0.6)^{2+|k|}}{0.078} - \frac{(0.3)^{2+|k|}}{0.0456} + \frac{(0.1)^{2+|k|}}{0.092} \quad \text{for } k < 0$$

Using this numerical formula and applying it to a forecasting horizon of $h = 3$, the normalized patterns $\mathbf{D}_k$ are:

$$\mathbf{D}_k = \begin{cases} \frac{1}{\delta_0}(\delta_{-1}, \delta_{-2}, \delta_{-3}) = \frac{1}{2.750}(2.188, 1.485, 0.944) = (0.796, 0.540, 0.343) & \text{for } k = 0, \\ \frac{1}{\delta_1}(\delta_0, \delta_{-1}, \delta_{-2}) = \frac{1}{2.200}(2.750, 2.188, 1.485) = (1.25, 0.995, 0.675) & \text{for } k = 1, \\ \frac{1}{\delta_2}(\delta_1, \delta_0, \delta_{-1}) = \frac{1}{1.760}(2.200, 2.750, 2.188) = (1.25, 1.562, 1.243) & \text{for } k = 2, \\ \frac{1}{\delta_3}(\delta_2, \delta_1, \delta_0) = \frac{1}{1.408}(1.760, 2.200, 2.750) = (1.25, 1.562, 1.953) & \text{for } k = h = 3. \end{cases} \tag{4.2}$$

Under appropriate regularity conditions, if during an extreme event the trajectory $\mathbf{X}_t$ is approximately collinear to $(\psi_1^m, \psi_1^{m-1}, \ldots, \psi_1, 1)$ with exponential growth rate $\psi_1^{-1} = 1.25$, then the forecasting probabilities are:

$$\mathbb{P}\left(\left\|\frac{\mathbf{X}_{t+h}}{|\mathbf{X}_t|} - s\mathbf{D}_k\right\| < \delta \middle| |\mathbf{X}_t| > x, \left\|\frac{\mathbf{X}_t}{|\mathbf{X}_t|} - s\boldsymbol{\psi}\right\| < \eta\right) \underset{x\to+\infty}{\longrightarrow} \begin{cases} \zeta_1^{\alpha k}(1 - \zeta_1^{\alpha}) & \text{if } k \in \{0, 1, \ldots, h-1\} \\ \zeta_1^{\alpha h} & \text{if } k = h \end{cases} \tag{4.3}$$

where $\boldsymbol{\psi} := (\psi_1^m, \psi_1^{m-1}, \ldots, \psi_1, 1)$ and $s \in \{-1, +1\}$ indicates the sign of the extreme event.

Given an observed trajectory (X_{t-2}, X_{t-1}, X_t) approximately collinear to $\boldsymbol{\psi} = (0.64, 0.8, 1)$, the forecaster computes the normalized observed pattern and matches it against the theoretical patterns $\{\mathbf{D}_0, \mathbf{D}_1, \mathbf{D}_2, \mathbf{D}_3\}$. With tail parameter $\alpha = 1.5$, the conditional forecasting probabilities are:

$$\mathbb{P}\left(\left\|\frac{\mathbf{X}_{t+h}}{|\mathbf{X}_t|} - s\mathbf{D}_k\right\| < \delta \middle| |\mathbf{X}_t| > x, \left\|\frac{\mathbf{X}_t}{|\mathbf{X}_t|} - s\boldsymbol{\psi}\right\| < \eta\right) \underset{x\to+\infty}{\longrightarrow} = \begin{cases} (0.8)^{1.5\times0}(1 - (0.8)^{1.5}) \approx 1 \times 0.284 = 0.284 & \text{for } k = 0 \\ (0.8)^{1.5\times1}(1 - (0.8)^{1.5}) \approx 0.716 \times 0.284 = 0.203 & \text{for } k = 1 \\ (0.8)^{1.5\times2}(1 - (0.8)^{1.5}) \approx 0.512 \times 0.284 = 0.145 & \text{for } k = 2 \\ (0.8)^{1.5\times3} \approx 0.367 & \text{for } k \geq 3 \end{cases}$$

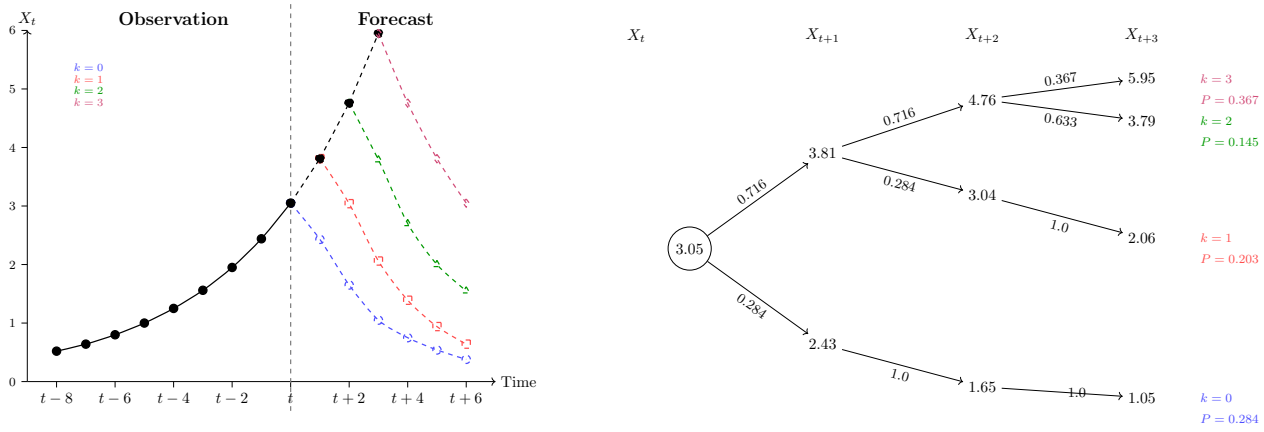

Figure 4: Pattern-based forecasting illustration for MAR(1,3) process with exponential growth observation and probabilistic forecast trajectories. Node values computed as $X_{t+h} = X_t \times D_k^{(h)}$ where D_k are normalized patterns from (4.2). Probabilities follow $P(k) = \zeta_1^{\alpha k}(1-\zeta_1^{\alpha})$ for $k \in \{0, 1, 2\}$ and $P(k = 3) = \zeta_1^{\alpha h}$ as in (4.3).

Figure 4 demonstrates the implementation of the theoretical framework where the left panel shows the transition from observed exponential growth to multiple forecasting scenarios, while the right panel presents the probability tree structure starting from $X_t = 3.05$ with computed conditional probabilities for different bubble peak timings ($k = 0, 1, 2, 3$). The visualization illustrates how the pattern-matching algorithm leverages the explicit MA(∞) coefficients to assign forecast probabilities based on the observed trajectory's alignment with the theoretical patterns $\mathbf{D}_k$, demonstrating the practical

utility of the coefficient formulas from Lemma 2.1 for systematic bubble forecasting through pattern recognition. During extreme events, the process dynamics simplify to geometric patterns governed by the noncausal root ζ_1, enabling tractable probabilistic forecasting of bubble peaks where each branch represents a distinct collapse scenario with its associated probability.

5 Conclusion

This note derives closed-form expressions for the MA(∞) coefficients of mixed causal-noncausal autoregressive MAR(r, s) processes through Laurent series expansion and residue calculus. Our results extend the partial fraction decomposition approach from the MAR$(1, 1)$ case to arbitrary MAR(r, s) specifications. The derived expressions enable exact simulation algorithms that avoid the truncation bias inherent in recursive methods, as demonstrated through numerical comparisons across different model specifications. Furthermore, the explicit coefficient structure facilitates the development of pattern-based forecasting methodologies for extreme events in processes with α-stable innovations.

Conflict of interest statement

The author has no conflicts of interest to declare.

Data availability statement

The figures in this article are generated using Python code; no real data is used, and all figures along with the Python code implementing the paper's formulas are available in the replication code package.

References

Ahlfors, L.V., 1979. Complex Analysis. 3rd ed., McGraw-Hill, New York.

Andrews, B., Calder, M., Davis, R., 2009. Maximum likelihood estimation for α-stable autoregressive process.

Blasques, F., Koopman, S.J., Mingoli, G., Telg, S., 2025. A novel test for the presence of local explosive dynamics. Journal of Time Series Analysis 46, 966–980.

Fries, S., 2022. Conditional moments of noncausal alpha-stable processes and the prediction of bubble crash odds. Journal of Business & Economic Statistics 0, 1–21.

Giancaterini, F., Hecq, A., Morana, C., 2022. Is climate change time-reversible? Econometrics 10.

Gourieroux, C., Jasiak, J., 2023. Generalized covariance estimator. Journal of Business & Economic Statistics 41, 1315–1327.

Gourieroux, C., Jasiak, J., Monfort, A., 2020a. Stationary bubble equilibria in rational expectation models. Journal of Econometrics 218, 714–735.

Gouriéroux, C., Jasiak, J., 2016. Filtering, prediction and simulation methods for noncausal processes. Journal of Time Series Analysis 37, 405–430.

Gouriéroux, C., Monfort, A., Renne, J.P., 2020b. Identification and estimation in non-fundamental structural varma models. The Review of Economic Studies 87, 1915–1953.

Gouriéroux, C., Zakoian, J.M., 2017. Local explosion modelling by non-causal process. Journal of the Royal Statistical Society: Series B (Statistical Methodology) 79, 737–756.

Hecq, A., Issler, J.V., Telg, S., 2020. Mixed causal–noncausal autoregressions with exogenous regressors. Journal of Applied Econometrics 35, 328–343.

Hecq, A., Telg, S., Lieb, L., 2017. Simulation, estimation and selection of mixed causal-noncausal autoregressive models: The marx package. SSRN https://ssrn.com/abstract=3015797.

Hecq, A., Velasquez Gaviria, D., 2025. Non-causal and non-invertible arma models: Identification, estimation and application in equity portfolios. Journal of Time Series Analysis 46, 325–352.

Lanne, M., Saikkonen, P., 2011. Noncausal autogressions for economic time series. Journal of Time Series Econometrics 3.

de Truchis, G., Fries, S., Thomas, A., 2025. Forecasting Extreme Trajectories Using Seminorm Representations. Working Paper 2025-06. Chaire Économie du Climat. Paris. Working Paper 2025-06.

Velasco, C., Lobato, I.N., 2018. Frequency domain minimum distance inference for possibly noninvertible and noncausal ARMA models. The Annals of Statistics 46, 555 – 579.